Shear-Enhanced Crystallization in Isotactic Polypropylene. 1. Correspondence between in Situ Rheo-Optics and ex Situ Structure Determination

Guruswamy Kumaraswamy, Ani M. Issaian, and Julia A. Kornfield*

Division of Chemistry and Chemical Engineering, California Institute of Technology, Pasadena, California 91125

Received May 18, 1999; Revised Manuscript Received July 15, 1999

ABSTRACT: The effects of "short term shearing" on the subsequent crystallization of a polydisperse Ziegler−Natta isotactic polypropylene are observed using in situ optical measurements and ex situ microscopy. Imposition of brief intervals of shear (0.25−20 s, less than a thousandth of the quiescent crystallization time) can reduce the crystallization time by 2 orders of magnitude (e.g., at 141 °C with a wall shear stress of 0.06 MPa). With increasing shearing time, the crystallization time saturates and highly anisotropic growth ensues. This transition to oriented growth correlates with changes in the transient behavior during flow and the semicrystalline morphology observed ex situ. During flow, we observe the generation of long-lived, highly oriented structures (evident in the transient birefringence) under all conditions that induce subsequent growth of highly oriented crystallites. In turn, the development of oriented crystallites observed in situ after cessation of flow correlates with development of a "skin-core" morphology (highly oriented skin on a spherulitic core) observed ex situ. Interestingly, the long-lived structures generated during flow appear at shorter times with increasing temperature (at fixed shear stress), the opposite of the trend one would expect on the basis of the temperature dependence of quiescent crystallization.

1. Introduction

Processing of semicrystalline polymeric resins strongly affects their final morphology and consequently their material properties. Semicrystalline polymers are often processed from the melt state. In common polymer processing operations such as injection molding, film blowing, and fiber spinning, the molten polymer is subjected to intense shear and elongational flow fields and crystallizes during or subsequent to the imposition of flow. The semicrystalline morphology that develops in the final product is typically very different from what is observed for quiescent crystallization of the same polymer. For example, the chain-extended crystals and the interlocked lamellar structure formed as polyethylene crystallizes under the influence of an elongational flow field yield materials with a very high modulus.[1−3] The high stresses and strain rates experienced by a hot polymer melt as it contacts the cold walls of the die in an injection molding operation can lead to the development of a highly nonuniform "skin-core" morphology. The difference in properties (such as crystallinity and degree of orientation) between the highly oriented crystallites in the skin and the spherulitic core can lead to undesirable effects such as stress whitening, warpage, or, in extreme cases, delamination of the skin. On the other hand, the skin can offer a desired hardness of the surface. Thus, an understanding of the nature of flow-enhanced crystallization with respect to the influence of processing conditions and resin characteristics is required to enable rational design of materials and to optimize properties.

The technological importance of the development of inhomogeneous semicrystalline structure developed during injection molding has driven extensive investigations of test specimens injection molded from various resins under different processing conditions.[4−11] Such studies have yielded a wealth of information regarding the details of processing−morphology relations for particular resins under specific processing conditions. However, the nonisothermal nature of molding and the complicated flow fields imposed makes it difficult to gain insight into the underlying dynamics that lead to the final observed morphology.

To separate the effects of flow from those of temperature transients and gradients present in injection molding, other researchers have used modified rheometers to study shear-enhanced crystallization under well-defined flow and isothermal conditions.[12−22] In most of these studies, the polymer melt was subjected to continuous shear at the crystallization temperature, and the onset and progress of crystallization were monitored using a variety of techniques. The following are the three main conclusions from these studies: (i) Shear was observed to accelerate crystallization kinetics and, under severe conditions, to change the semicrystalline morphology from spherulitic to crystallites oriented in the flow direction. (ii) While researchers recognized the difficulty in separating the process of crystal growth from nucleation,[19] they attributed the enhancement in crystallization kinetics to an increase in nucleation rate caused by distortion of polymer chains in the melt (based on studies of nucleation density,[20] induction time for nucleation,[19] and crystal growth rates). (iii) A pronounced effect of molecular weight and molecular weight distribution was observed,[15,17,19,20,22] and it was suggested that the high molecular weight species played an important role in melt orientation and the observed enhancement in crystallization kinetics. However, most of these experiments did not access conditions typical of industrial processing limited to relatively low stress, strain rate, or total strain. In addition, the imposition of continuous shear during crystallization changes the orientation distribution of crystallites due to reorientation in the shear field, making it difficult to differ-

10.1021/ma990772j CCC: $18.00
Published on Web 10/07/1999

entiate between the formation of oriented crystallites and their reorientation due to flow.

A new experiment was proposed by Janeschitz-Kriegl and co-workers[23] in the early 1990s to address some of the limitations in prior experimental approaches. They studied the effect of brief, intense shearing of an isothermal polymer melt (brief compared to the time taken for crystallization) on subsequent crystallization. This approach aimed to separate the effect of primary nucleation (which was assumed to happen mainly during shear) from the growth of crystals at later times. Reorientation of crystallites in the flow field was also minimized. A well-defined thermal history was applied and high wall shear stresses were imposed for controlled durations.

In polydisperse isotactic polypropylenes, they found that (i) a brief "pulse" of shear can cause rapid subsequent growth of highly oriented crystallites and (ii) the effect of a shear "pulse" on the crystallization time scaled with the fourth power of the wall shear strain rate and the second power of the shearing time, $\dot{\gamma}_w^{-4} t_s^{-2}$. To explain this scaling, a model with an Avrami-like phenomenology was put forward with an arbitrary shear rate dependence assigned to the nucleation rate and to the growth rate of the "threadlike" precursors[23] that were assumed to grow from the point nucleation sites during shear. The model also explained the weaker dependence of crystallization time on shear rate and shear time for nucleated isotactic polypropylene ($\dot{\gamma}_w^{-2} t_s^{-1}$). Resins with a lower content of high molecular weight chains also showed this weaker scaling, which they could explain by assuming that the number of nuclei is fixed rather than increasing due to sporadic generation during shear.[24] However, while the model is very successful in describing their results, there is no molecular explanation for the nature of the "threadlike" precursors that form the basis of the theory. Finally, it must be noted that $\dot{\gamma}_w^{-2} t_s^{-1}$ is not dimensionless but is rendered dimensionless in the model by an arbitrary factor, g, having units of time.

Other phenomenological approches to modeling have relied on modifications to the Avrami formalism.[25−28] An early model by Ziabicki[25,26] formulated a general approach to crystallization from an oriented state by modifying the Avrami nucleation and growth rates to be functions of a time dependent "orientation characteristic". Recent work by McHugh and co-workers[27,28] further introduces concepts of irreversible thermodynamics and employs more accurate rheological models for the amorphous and partially crystalline states. Their model is very sensitive to the coupling between the degree of crystallinity, the orientation of the crystalline phase and the anisotropy of the amorphous phase subject to flow. This model appears promising, but the molecular variables that govern these coupling parameters need to be understood before it can be used predictively.

An earlier "zero-parameter" approach to theoretically explaining flow-induced crystallization used the thermodynamic concept of melting point elevation.[29,30] This approach, originally proposed by Flory[29] to explain strain-induced crystallization in cross-linked rubbers, relates the reduced entropy of the oriented state from which the polymer crystallizes to an elevation in the equilibrium melting point of the crystal. It was hypothesized that this caused a given temperature to correspond to a deeper subcooling, which causes the observed enhancement in the crystallization kinetics. This theory does not attempt to explain how flow-enhanced crystallization often results in the development of oriented semicrystalline morphologies. Further, experimental evidence suggests that the calculated increase in the equilibrium melting point is too small to account for the observed enhancement in crystallization kinetics.[12,31,32] However, Andersen and Carr[17] have suggested that the observed crystallization kinetics may be reconciled with the thermodynamic theory by accounting for the effect of the high molecular weight tail of the chain length distribution on the decrease in entropy upon shearing.

Development of reliable models for flow-enhanced crystallization requires experimental data on the earliest events that occur during flow and their relationship to subsequent crystallization kinetics and morphology obtained using a protocol that separates the effects of flow from those of thermal transients or gradients (viz., the protocol developed by Janeschitz-Kriegl and co-workers). Insights into the interplay of flow and crystallization can be obtained by following the development of order at different length scales in real time using in situ probes of structure. In the next section, we briefly describe instrumentation developed in our laboratory that generates controlled thermal and flow histories by imposing a transient deformation at well-defined stress for a set duration. In situ structural probes that record the formation of structure in real time are incorporated into our instrument to provide information about the initial stages of the transformation during shear and the crystallization process at longer times after cessation of flow. In light of Janeschitz-Kriegl's findings and their model, it is of immediate interest to determine the prerequisites for inducing oriented growth: Is there a critical shear stress that needs to be applied? What is the duration for which it needs to be applied? What occurs during flow that leads to subsequent oriented growth? How are the dynamics of these flow-induced events affected by thermodynamic factors (e.g., subcooling) vs dynamic factors (e.g., the relaxation spectrum of the melt)? Here we begin to address these questions by examining a polydisperse, industrial isotactic polypropylene sample similar to the one used by Janeschitz-Kriegl and co-workers. We compare our data with the available literature on polydisperse polymers and concentrate on structure development during shear, correlating it with the anisotropic structure development at later times as the polymer crystallizes.

2. Experimental Section

We have constructed an instrument that retains the essential features of the protocol pioneered by Janeschitz-Kriegl and co-workers[23] (well-defined flow and thermal history, high shear stresses, and short shearing times to minimize flow-induced reorientation of crystallites) and confers two additional advantages: it is able to work with relatively small amounts of material and is designed to facilitate in situ structural characterization using a variety of techniques.[33] Our instrument employs pressure-driven flow to achieve wall shear stresses on the order of 0.1 MPa for durations that can be precisely controlled from 100 ms to several minutes. A slit geometry (slit width = 0.5 mm) with a large aspect ratio (∼10) is used to generate a simple two-dimensional flow profile. Isothermal conditions can be maintained at the sample with stability to about ±0.1 °C for the duration of the experiment.[34] To open the way to studying model systems, our device requires only small amounts of sample (a set of experiments can be done with about 10 g of material with each experiment

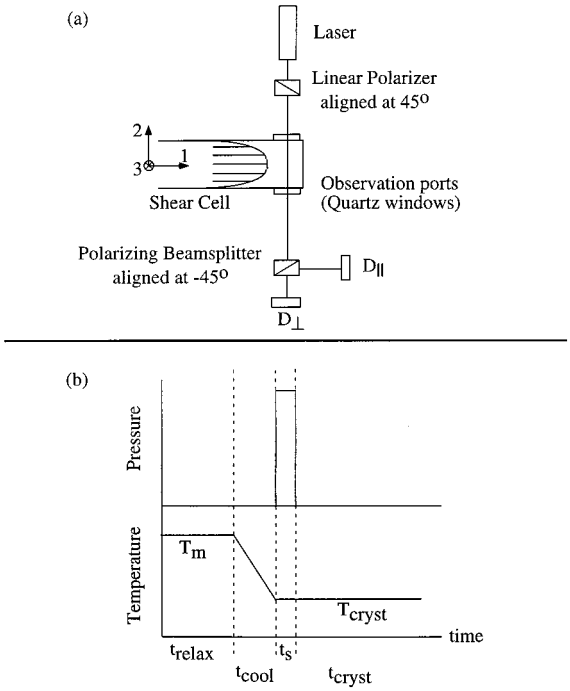

Figure 1. Schematic of the optical train used for turbidity and birefringence measurements. P1 is a linear polarizer oriented at 45° to the flow direction, P2 is a polarizing beam splitter. The extraordinary beam from P2 is incident on detector $D_{||}$, which reads the intensity of light ($I_{||}$) through parallel polarizers. The through beam is incident on detector $D_{\perp}$ which reads the intensity of light ($I_{\perp}$) through perpendicular polarizers.

using about 0.5 g). The instrument facilitates use of a variety of structural probes (turbidity, birefringence, SALS, SAXS, WAXD, IR dichroism) to obtain real-time, in situ information about the evolution of structure in the melt and as the polymer crystallizes. The sample can be extracted at the end of an experiment and rapidly quenched by plunging into ice water for ex situ examination. A Reichert UltraCut S Cryomicrotome has been used to section the sample at a temperature of −100 °C. Sections, 5 μm in thickness, are obtained in the flow−gradient (1−2, axes defined in Figure 1) and the gradient−vorticity (2−3) planes for optical microscopy. Results of turbidity and birefringence measurements and ex situ polarized optical microscopy are presented here (optical arrangement shown in Figure 1a). The corresponding in situ and ex situ synchrotron X-ray scattering experiments will be presented separately.

We examine shear-enhanced crystallization in a polydisperse Ziegler−Natta isotactic polypropylene, PP-300/6 ($M_w \sim$ 300 000 g/mol, PDI ∼ 6−8, pentad content [mmmm] ∼96%, melt flow index = 12 dg/min at 230 °C/2.16 kg load). In all these experiments, polymer melt held in a reservoir maintained at 180 °C was injected into a hot slit die. The die, which is thermally isolated from the reservoir, was held at a high temperature (220 °C for 5 min)[35] to erase the memory of the filling process and then cooled to the desired crystallization temperature, T_{cryst} (Figure 1b). The crystallization temperature was selected such that the time for quiescent crystallization is much greater than the time required to cool the die (typically around 10 min). Care was taken to minimize temperature undershoots during cooling. The stability of T_{cryst} was optimized to only about ±0.5 °C since we found that the sensitivity of our shear-enhanced crystallization results to temperature fluctuations was not as high as might be expected from quiescent crystallization studies.

The relaxed, isothermal subcooled polymer melt is subjected to intense shearing at wall shear stresses, σ_w, of 0.03 and 0.06 MPa for brief shearing times (short enough that no turbidity is evident). Start-up and cessation of shearing takes ∼20 ms, giving a boxlike wall shear stress profile.[36] The polymer was allowed to crystallize subsequently, and the turbidity and birefringence were tracked to monitor the progress of crystallization. The wall shear stress, σ_w, is computed from the measured pressure drop across the slit. We do not present our data in terms of a calculated wall strain rate, $\dot{\gamma}_w$, or strain, γ_w, because we do not know how the rheological properties change due to the ordered structure that forms during the shearing time (see Results).

Light from a 15 mW HeNe (λ = 632.8 nm) laser polarized at 45° to the flow direction passes through the sample and is analyzed using a polarizing beam splitter with its axis at −45° to the flow direction (Figure 1a). Detectors $D_{\perp}$ and $D_{||}$ measure the intensity of light through crossed and parallel polarizers, $I_{\perp}$ and $I_{||}$, respectively. The sum of the intensities incident on the the two detectors ($D_{\perp}$ and $D_{||}$) is I_{tot} ($=I_{\perp} + I_{||}$), the total light transmitted through the sample. The total intensity normalized by the intensity of light transmitted initially through the molten sample, $I_{tot}(t=0)$, decreases as crystallites that scatter light form. When depolarization can be neglected, $I_{\perp}/I_{tot}$ is related to the birefringence, Δn (eq 1), and is a measure of the anisotropy in the sample

$$\Delta n = \frac{\lambda}{\pi d} \arcsin \sqrt{\frac{I_{\perp}}{(I_{||} + I_{\perp})}} \qquad (1)$$

where λ is the wavelength of light and d is the thickness of the sample. Depolarization is negligible when little scattering occurs; since the total transmitted intensity never drops significantly during the shear "pulse", this equation can be used to describe the orientation of the polymer during flow.

The optics were calibrated at the beginning of each experiment to adjust for the different sensitivity of the detectors by using a quarter wave plate with its axis along the flow direction. Data is acquired with high time resolution (5−20 ms) during shearing to characterize the anisotropy in the melt. After cessation of shear, structure evolution occurs on much longer time scales, so lower data acquisition rates (depending on the characteristic crystallization time) are used subsequently.

3. Results

In this section, we present our results on the shear-enhanced crystallization in PP-300/6 as a function of shearing time and wall shear stress. First, we examine the effect of shear on the time scale for crystallization, then we describe the development of orientation as determined by our in situ birefringence measurements as the polymer crystallizes. Next, we present ex situ measurements that show how "extreme" shearing conditions (high wall shear stress and shearing time) lead to the development of a pronounced "skin-core" morphology. We will demonstrate that an unusual rheo-optical signature observed *during* short-term shearing correlates with the subsequent formation of anisotropic semicrystalline texture. Finally, we show that the dynamics of creation of this oriented structure during flow is controlled by relaxation dynamics of the melt rather than by the degree of subcooling.

In situ optical techniques provide information about structure formation averaged over the thickness of the flow channel. Simple rheo-optical measurements such as monitoring the turbidity as the sample crystallizes have been used to follow the progress of crystallization. Shearing PP-300/6 at a wall shear stress of 0.06 MPa at a temperature of T_{cryst} = 141 °C accelerates the crystallization kinetics (Figure 2) and the sample becomes turbid in a very short time compared to quiescent crystallization. The onset of turbidity is due to the material most strongly influenced by the flow history,

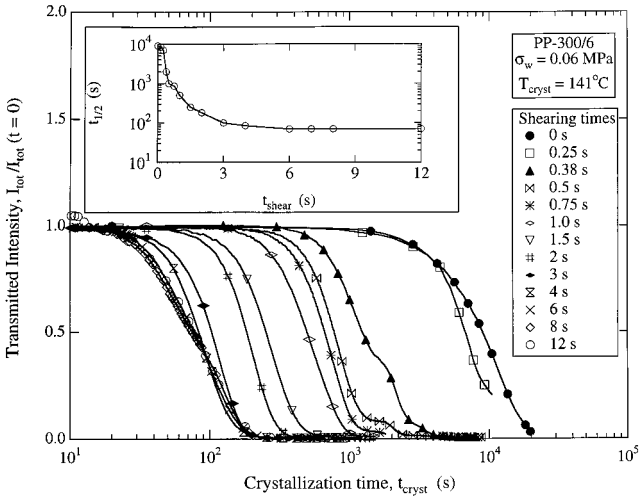

Figure 2. Turbidity of PP-300/6 as it crystallizes following a "pulse" of shear at T_{cryst} = 141 °C and σ_w = 0.06 MPa for various shearing times, t_s, ranging from 0 to 12 s. The lines indicate experimental data; symbols are sparsely distributed on the lines to identify the experiments at different shearing times. Scattering of incident light as the polymer crystallizes leads to increased turbidity. The crystallization time decreases with increased shearing time, and the crystallization half time, $t_{1/2}$ (see text), reaches a plateau after a shearing time of about 5 s (inset).

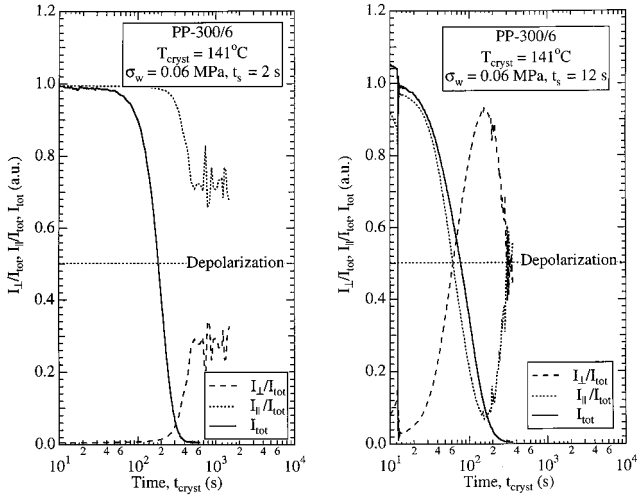

Figure 3. (a) Relative intensity through crossed and parallel polarizers for PP-300/6 as it crystallizes following a "pulse" of shear at the same T_{cryst} and σ_w as in Figure 2 (T_{cryst} = 141 °C, σ_w = 0.06 MPa). t_s = 2 s does not cause a significant increase in the normalized intensity between crossed polarizers, $I_\perp/I_{tot}$, until multiple scattering gives rise to depolarization. (b) Longer shearing times (t_s = 12 s) lead to the birefringence going "over orders", indicating the formation of a highly oriented crystalline structure.

typically the material near the walls which experiences the highest shear rate. We define a characteristic crystallization time, called the "half-time", $t_{1/2}$, as the time taken for the transmitted intensity to decrease to half its initial value. This half-time is not to be confused with the time taken to achieve a degree of crystallinity of 0.5, since the transmitted intensity can drop to zero when only a small amount of material in thin layers near each wall becomes opaque. Further, a given transmittance does not generally correspond to a given degree of crystallinity since it is sensitive to the size and shape of the crystalline scatterers. The crystallization temperature, T_{cryst}, was selected such that $t_{1/2}$ for quiescent crystallization was on the order of a few hours. Upon shearing the melt for ~4 s, the half-time decreases by about 2 orders of magnitude (Figure 2, inset). As the shearing time is increased, the crystallization time first decreases rapidly and then reaches a plateau at a shearing time of about 5 s (Figure 2, inset). The geometry of the shear cell limits us to a maximum strain of about 100, which restricts us to shearing times $t_s \leq$ 12 s for PP-300/6 at this σ_w and T_{cryst}.

As the polymer crystallizes, $I_{tot}(t)/I_{tot}(0)$ drops, $I_\perp/I_{tot}$ rises, and $I_\parallel/I_{tot}$ falls. Even in the case of unoriented crystallization, multiple scattering gives rise to depolarization manifested in an increase in $I_\perp/I_{tot}$ and a decrease in $I_\parallel/I_{tot}$.[37] This change is not indicative of birefringence; it is observed even in quiescent crystallization when the structure is isotropic. For example, as PP-300/6 crystallizes at 141 °C after shearing for 2 s at σ_w = 0.06 MPa, the increase in the normalized intensity between crossed polarizers, $I_\perp/I_{tot}$, occurs mainly after the the total transmitted intensity $I_{tot}(t)/I_{tot}(0)$ drops to less than 0.1 (Figure 3a). Polarized light microscopy with crossed polarizers (PLM-CP) shows that the sample quenched into ice water at the end of the crystallization experiment (viz., when the sample turns completely turbid, $t_{cryst} \sim$ 1800 s) contains no visible oriented crystallites and no skin-core texture (Figure 4a,b). Large spherulitic structures, about 40 μm across, are observed in a 100 μm region near the walls in both flow−gradient (1−2, axes defined in Figure 1) and gradient−vorticity (2−3) planes while smaller spherulites are observed through the rest of the sample (characteristic of crystallization occurring during the quench).

Qualitatively different behavior is seen in $I_\perp/I_{tot}$ for shearing times longer than about 5 s. For example, when the polymer crystallizes after being sheared for 12 s (at the same T_{cryst} and σ_w), $I_\perp/I_{tot}$ starts increasing immediately (before the total transmitted intensity has dropped by even 10%) and goes through a maximum (Figure 3b). The birefringence going "over orders" indicates the formation of highly oriented crystallites. This is evident in the skin-core morphology observed in the optical micrographs (PLM-CP, Figure 4c,d) of microtomed sections of the sample quenched after it became completely turbid (viz., at $t_{cryst} \sim$ 400 s). The micrograph of the sample viewed in the flow−gradient (1−2) plane shows a bright "skin" region near the walls of the die which, when viewed in the gradient−vorticity (2−3) plane, appears dark. This suggests that crystallites having cylindrical geometry are oriented along the flow direction in the skin region. The bright skin region extends to a depth of about 55 μm from the wall. The material appears stratified with a "fine-grained" layer (~100 μm) between the skin and the isotropic core. Since the shear stress in the sample drops linearly from a maximum at the wall (σ_w = 0.06 MPa) to zero at the center of the flow channel, the "critical" shear stress at the boundary of the skin and the "fine-grained" layer can be calculated to be $\sigma_{crit} \approx$ 0.047 MPa.

The central core region exhibits spherulitic structures (Figure 4c,d) which are much smaller than those observed during quiescent crystallization at 141 °C (several 100 μm in diameter; micrographs not presented). Near quiescent conditions prevail over the central core, since this polymer exhibits shear thinning behavior that results in a flattened velocity profile.[38] Since the quiescent crystallization kinetics for PP-300/6

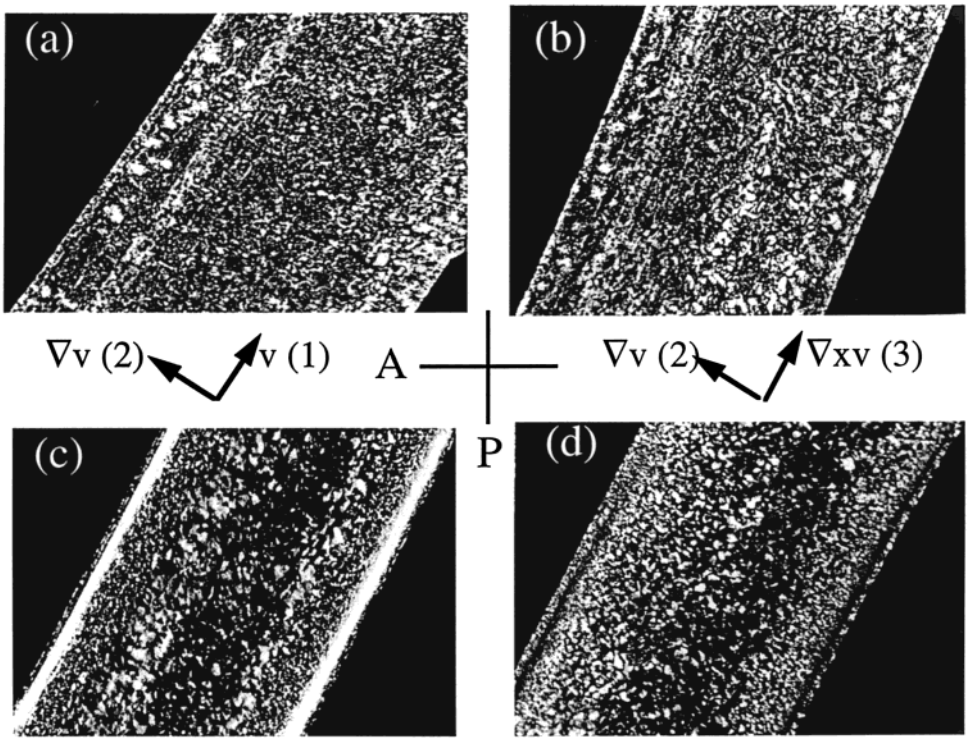

Figure 4. Micrographs (PLM-CP) of PP-300/6 crystallized at T_{cryst} = 141 °C after shearing at a wall shear stress of 0.06 MPa for t_s = 2 s (a and b) and t_s = 12 s (c and d) at the same experimental conditions as in Figure 3. The polarizer and analyzer directions are at ±45° to the long axis of the sample, as indicated. Images on the left show the flow−velocity gradient (1−2) plane, while those on the right show the velocity gradient−vorticity (2−3) plane. After short shearing intervals (t_s = 2 s), no oriented structures are visible (a and b). Sufficiently long shearing times (t_s = 12 s) induce the formation of a characteristic skin-core morphology. The oriented skin region appears bright when viewed down the neutral direction (c) and dark when viewed down the flow direction (d) indicating that the skin has crystallites with cylindrical symmetry.

at 141 °C is known to be slower than the time scale allowed for crystallization in the shear-enhanced crystallization experiments (quenched at t_{cryst} = 400 s and 1800 s for t_s = 12 s, 2 s vs 20 000 s for quiescent conditions), we infer that the spherulites in the inner core regions (Figure 4) formed during the ice water quench.[39]

The enhancement in crystallization kinetics is manifested in the change in $t_{1/2}$ with shearing time, while the development of oriented semicrystalline structures is reflected in the time at which $I_\perp/I_{tot}$ goes through a maximum. The optical signals are indicative mainly of structure formation near the walls of the die, since the polymer there crystallizes before the region near the center as a result of experiencing high shear rate and strain. The initial decrease in $t_{1/2}$ with increasing t_s shows intermediate behavior between the two power laws previously observed for short-term shearing experiments on a similar iPP[23,24] (Figure 5). Maxima in $I_\perp/I_{tot}$ during crystallization are only observed for t_s > 5 s; in this regime, both the time to reach these maxima, $t_{\lambda/2}$, and $t_{1/2}$ do not change with t_s.

To gain insight into the origin of the differences in the degree of orientation observed in the final crystallized samples, we examine the melt birefringence during shear (Figure 6). As the polymer melt is sheared, the isotropic conformation of the macromolecules is distorted, giving rise to birefringence,[40] Δn (Figure 6, bottom). Since the chain stretching is small relative to full extension under our experimental conditions,[40] the stress−optic rule applies at short times where no crystallization occurs. Under such conditions, the birefringence can be related to the third normal stress difference, N_3 (=$\sigma_{11} - \sigma_{33}$, where 1, 2 and 3 represent the flow, gradient and vorticity directions). The high shear stresses imposed on the polymer in the experiments result in the nonlinear overshoot observed in the birefringence on start-up of flow (Figure 6, bottom). Since $\sigma_{22} - \sigma_{33}$ is small,[41] N_3 follows the same behavior of the first normal stress difference, N_1 (=$\sigma_{11} - \sigma_{22}$). Overshoots in N_1 have been observed on shear start-up for solutions of polybutadiene[42] and have been rationalized in terms of the stretching of polymer chains in the

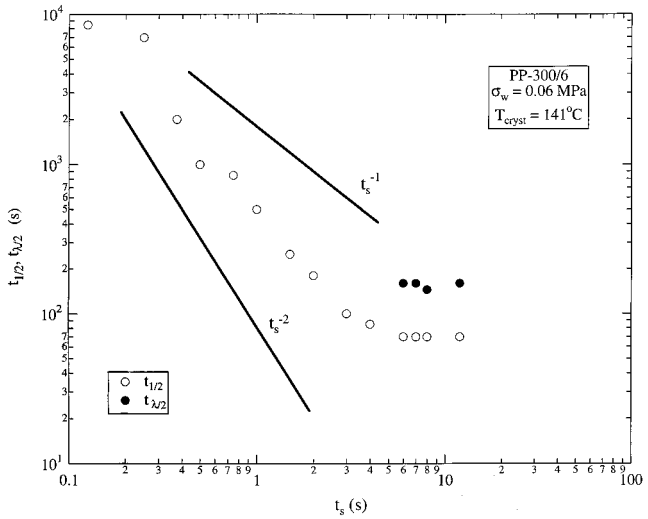

Figure 5. Turbidity half time, $t_{1/2}$, and time scale for formation of oriented structures, characterized by the time at which a maximum in $I_\perp/I_{tot}$ develops, $t_{\lambda/2}$ as a function of shearing time, t_s. Note that both these time scales saturate above a critical value of the shearing time, t_{crit}.

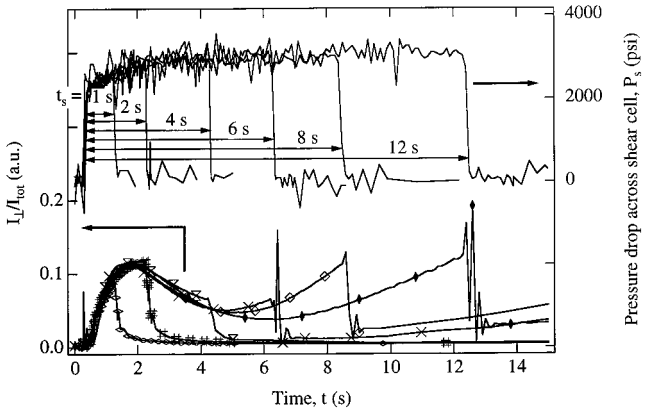

Figure 6. Transient intensity transmitted through crossed polars during shear pulses at the same T_{cryst} and σ_w as Figures 2−5. The top part of the plot shows the pressure imposed across the shear cell to turn the flow on and off. The imposed pressure drop (and corresponding wall shear stress) reaches 80% of the targeted value within 40 ms, gradually reaching the set value over the first 2 s and falls to zero within 40 ms, when the actuator is switched off. This provides a good approximation to a "boxlike" profile. The bottom part of the plot shows the corresponding birefringence traces for the experiments at different shearing times. The formation of the nonlinear overshoot is evident at about 2 s. Later, at times where a melt would have reached its steady state birefringence, there is a further upturn in the birefringence, which does not relax to zero after cessation of flow.

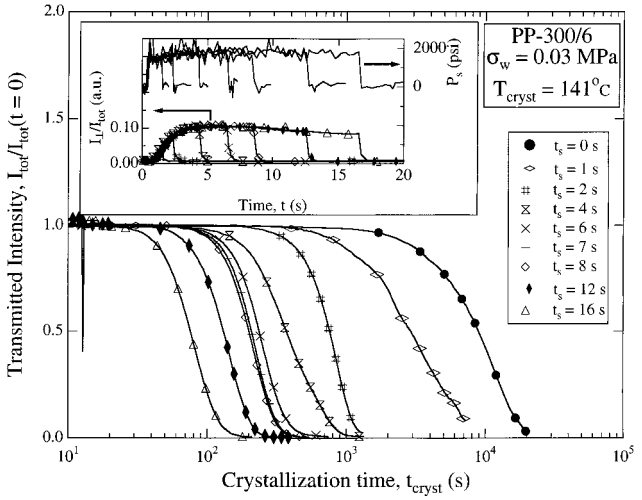

Figure 7. Shearing at a lower shear stress (0.03 MPa) at the same temperature (141 °C causes an acceleration in the crystallization kinetics, but no upturn is observed in the birefringence trace during shear (inset).

flow. Thus, this chain stretching also gives rise to the overshoot in N_3, which leads to the observed overshoot in the birefringence. After the initial start-up behavior, polymer melts show a steady state behavior and N_3 reaches a plateau. Another characteristic of melt behavior is that the birefringence relaxes back to zero upon cessation of shear. This is observed for $t_s < 5$ s (Figure 6).

Deviations from melt behavior both in the shape of the transient birefringence during flow and its relaxation after cessation of flow are observed with increasing shearing time. There is a transition from transient birefringence characteristic of melt flow to one that has a significant contribution due to long-lived, oriented structures generated during shear. For longer shearing times, the birefringence develops an upturn at times where the melt would show steady-state N_3. This upturn increases monotonically during the shear pulse, indicating the formation of an oriented structure which we call the "shear-induced structure".[43] Upon cessation of shear, the birefringence does not decay to zero but drops to a finite value and then increases with time. The development of the upturn in the birefringence during shear, which we associate with the formation of the "shear-induced structure", correlates with the development of strong anisotropy manifested by maxima in $I_\perp/I_{tot}$ observed at longer times as the polymer crystallizes and with the formation of a skin-core morphology in the crystallized sample. Real time synchrotron WAXD studies[44] during shear ($t_s > 5$ s) reveal oriented fiberlike crystalline reflections corresponding to the α-crystalline form of isotactic polypropylene.[45]

To examine the wall shear stress dependence of the "shear-induced structure", we sheared PP-300/6 at the same crystallization temperature, 141 °C, at a wall shear stress of $\sigma_w = 0.03$ MPa (0.03 MPa $< \sigma_{crit}$) for shearing times up to 20 s. The total shear strain experienced by the polymer at the longest shearing times under these conditions (estimated by weighing the polymer extruded during shear) was comparable to the strain experienced on shearing at $\sigma_w = 0.06$ MPa for 12 s. Shearing was again observed to accelerate the crystallization kinetics (Figure 7). A smaller overshoot in the melt birefringence (as compared to the experiments at higher σ_w) was observed during start-up of flow (Figure 7, inset). No upturn in the birefringence during shear was observed even for the highest shearing time, $t_s = 20$ s, where the instrumental limit of maximum accessible strain = 100 was reached. During crystallization only a very small increase in birefringence was evident in $I_\perp/I_{tot}$ and $I_\parallel/I_{tot}$. Ex situ polarized light microscopy of microtomed sections of the sample crystallized after shearing for 20 s showed no evidence of an oriented skin-core structure (Figure 8).

The effect of crystallization temperature was examined by studying shear-enhanced crystallization at a higher temperature, $T_{cryst} = 150$ °C. Crystallization experiments at 150 °C, at $\sigma_w = 0.06$ MPa showed the same trend as experiments at the lower crystallization temperature and the same wall shear stress: the crystallization kinetics was accelerated as the polymer was sheared, and the formation of oriented skin-core crystalline structures in the crystallized samples was found to correlate with formation of the "shear-induced structure" during shear (data not presented). As expected, the quiescent crystallization kinetics at 150 °C was slower than at $T_{cryst} = 141$ °C by about an order of magnitude. The "shear-induced structure", however, appeared at about the same shearing time as observed at $T_{cryst} = 141$ °C (about $t_s \sim 5$ s), suggesting that its formation might be controlled by the relaxation dynamics of the melt.

To examine this unanticipated temperature dependence of the formation of the "shear-induced structure", we examined the response of PP-300/6 to short-term shearing at various temperatures (Figure 9). At higher temperatures, viz. at lower undercoolings, the upturn in the birefringence developed at *shorter* shearing times (Figure 9a). The "shear-induced structure" is observed even at temperatures as high as 175 °C (above the nominal melting temperature of about 172 °C). The time axis for each experiment was rescaled by dividing by a temperature dependent "shift factor", $a'_T(T_{cryst})$ such that the upturn in the birefringence occurred at the

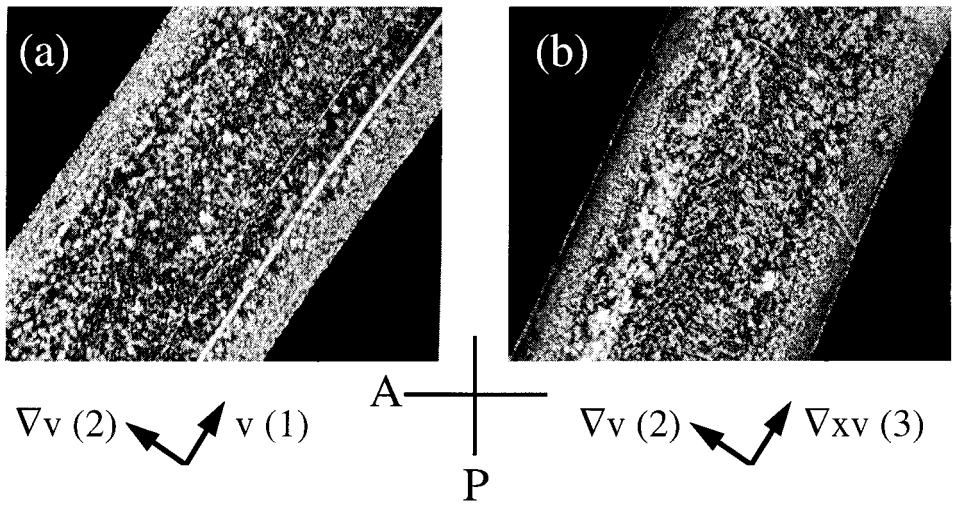

Figure 8. Micrographs (PLM-CP) in the (a) flow−velocity gradient (1−2) and (b) gradient−vorticity (2−3) planes for PP-300/6 sheared at 0.03 MPa at T_{cryst} = 141 °C for 20 s.

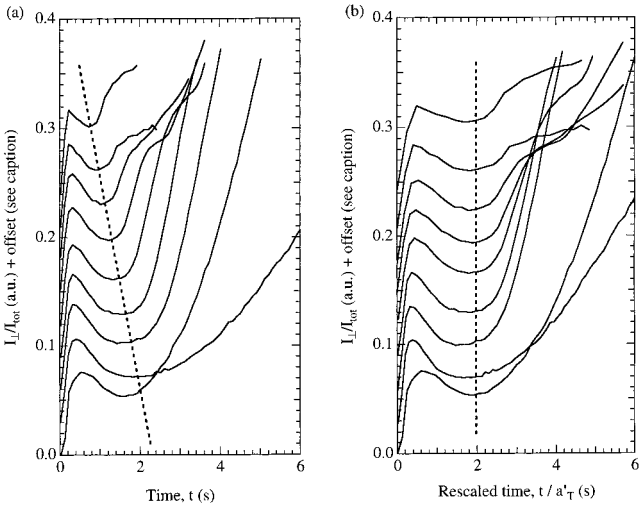

Figure 9. Temperature dependence of the "shear-induced structure" is manifested in the birefringence traces during shear shown as a function of (a) time and (b) rescaled time using a shift factor, a'_T, to superimpose the upturn in the birefringence. The curves represent experiments at 135, 140, 145, 150, 155, 160, 165, 170, and 175 °C, starting from the bottom. The magnitude of the initial transient overshoot in $I_\perp/I_{tot}$ overlaps to within 25% with the peak height decreasing with increasing temperature; the curves are vertically offset for clarity.

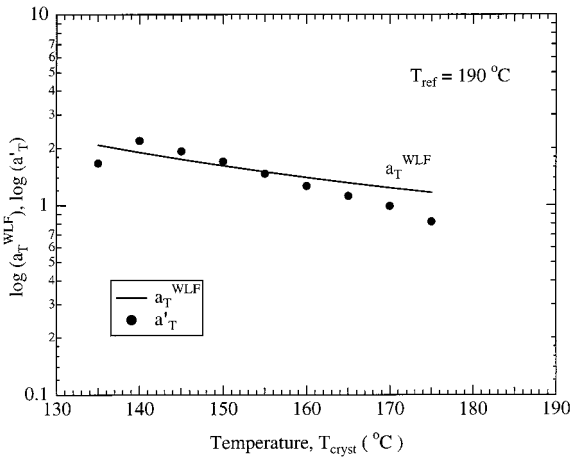

Figure 10. The temperature dependent shift factor, a'_T (filled circles) decreases with temperature in a manner similar to the literature value of the rheological shift factor, a_T^{WLF} (solid curve) for isotactic and atactic polypropylene.

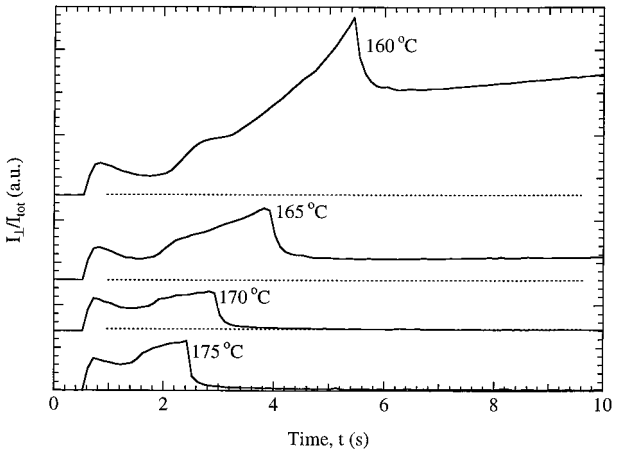

Figure 11. The intensity of light through crossed polarizers during shearing at σ_w = 0.06 MPa to approximately 100 strain units at the wall and after cessation of flow. Note that the birefringence observed during shear decays completely after shear cessation only at temperatures higher than 170 °C.

same rescaled time (Figure 9b). This "shift factor" decreases with increasing temperature (Figure 10) (while a characteristic quiescent crystallization time such as the induction time increases exponentially with T_{cryst}) and is remarkably similar to the established rheological shift factors for isotactic and atactic polypropylene.[46,47]

Upon cessation of shear, the "shear-induced structure" decays to a nonzero value at temperatures below 170 °C (Figure 11), while it decays completely for temperatures of 170 °C and above. These "melt" shearing experiments and the formation of the "shear-induced structure" were found to be far less sensitive to temperature fluctuations during the experiment than might be expected for crystallization at low subcoolings. Thus, reproducible results were obtained even with the ±1 °C level of temperature stability and uniformity of our apparatus. While the overall shape of the birefringence traces is robust, details such as the inflection in the experimental trace at 160 °C (Figure 11) were sensitive to subtle changes in experimental conditions (perhaps temperature variations in the shear cell).

4. Discussion

Our discussion is organized around the essential and interesting features evident in the behavior of this isotactic polypropylene and their implications in relation to current models of shear enhanced crystallization:

(i) There is a qualitative change in behavior with increasing shear stress and shearing time: below a critical stress and shearing time, shear decreases the time for crystallites to form; for $\sigma_w > \sigma_{crit}$ and $t_s > t_{crit}$, shear further induces highly anisotropic growth (skin-core structure).

(ii) The effect of shearing time on crystallization kinetics saturates for $t_s > t_{crit}$; further increase in t_s does not significantly reduce $t_{1/2}$ or $t_{\lambda/2}$.

(iii) The formation of skin-core morphology correlates with the growth of a birefringent feature ("shear-induced structure") during shear.

(iv) The time at which the "shear-induced structure" develops decreases with temperature and scales with the rheological shift factor for iPP.

(v) The "shear-induced structure" is observed to persist after the cessation of shear for temperatures below 170 °C.

Prerequisites for Induction of Highly Oriented Crystallization. The effect of flow changes with increasing strength and duration. Initially, application of a short interval of shear decreases the time for crystallites to grow, manifested by the decrease in the turbidity half-time (Figures 2 and 4). This qualitative behavior is observed at all levels of wall shear stress and at all subcoolings that we have examined. However, this initial change in the rate of crystallization is not accompanied by highly anisotropic growth (Figures 3 and 4). Ex situ optical micrographs (PLM-CP) [of sections subjected to a given shear history (σ_w, t_s, T_{cryst})] provide a way to examine the effect of shear stress, since the local shear stress varies linearly from σ_w at the wall to zero at the center. These images show that with increasing stress level at fixed t_s, shearing first appears to increase the crystallite nucleation density; if the shear stress is high enough and the duration long enough, then there is a fairly abrupt transition to highly oriented growth in a region near each wall.

This abrupt transition suggests that there is a critical stress below which highly oriented growth is not observed for a given shearing time. This threshold occurs at approximately 0.047 MPa for the example shown in Figure 4c,d. In accord with this estimate of the threshold stress, when a wall shear stress below this value is used, crystallization occurs at shorter times than quiescent (Figure 7), but highly oriented growth is not observed (behavior like that in Figure 3a) for any accessible duration of shear (limited by the 100 strain unit maximum for our instrument). The peculiar upturn in the birefringence during shear is also absent (inset, Figure 7). Correlated with the lack of oriented growth, the skin-core morphology is absent (Figure 8). Thus, the development of the "shear-induced structure" which correlates with subsequent oriented crystallization is observed only when the wall shear stress exceeds a critical value, viz. $\sigma_w > \sigma_{crit}$, *and* the shearing time exceeds a critical value which is a function of the imposed shear stress, viz. $t_s > t_{crit}(\sigma_w)$.

Requirement of a threshold strain for oriented crystallization has been reported by McHugh and co-workers,[32,48] who studied the development of crystallinity and orientation in an HDPE droplet subjected to an elongational ("strong") flow field. An acceleration of the crystallization kinetics by 2−3 orders of magnitude was observed. In situ measurements of birefringence and dichroism during and after cessation of flow indicated that the orientation developed in the system led to oriented crystallization, provided a critical strain was exceeded. Our experiments with shear flow show an acceleration in crystallization kinetics similar to that observed in McHugh's planar extension experiments. Also, the threshold criterion for a critical shearing time is equivalent to the requirement of a threshold strain for experiments done at a fixed shear stress above σ_{crit}. Thus, accelerated kinetics, development of oriented growth, and the existence of a "threshold" strain for oriented crystallization are observed both in "weak" shear flow experiments and "strong" extensional flows and appear to be general to different flow fields and polymer systems. Further, the ability to explore different shear stress levels opens the way to examining factors that control the critical strain. Results at $\sigma_w = 0.06$ and 0.03 MPa indicate a very nonlinear dependence of the threshold strain on the stress; the threshold is readily reached at 0.06 MPa, but inaccessible at 0.03 MPa, given our 100 strain unit limitation.

Saturation Behavior of "Skin" Crystallization Kinetics and Morphology. The optical signatures of the flow-induced, oriented growth exhibit an interesting saturation behavior. Once the shearing time exceeds 5 s (at 141 °C using $\sigma_w = 0.06$ MPa), longer durations of shear no longer reduce $t_{1/2}$. These durations of shear are long enough to cause sufficiently oriented growth to determine a time at which the retardation reaches $\lambda/2$; interestingly, the saturation behavior for $t_{1/2}$ also holds for the time required to reach a retardation of $\lambda/2$ (Figure 5). Both the turbidity and birefringence are dominated by a thin region near each wall (once this outermost layer extinguishes the transmitted beam, the turbidity is insensitive to subsequent build up of scatterers in the interior). The lack of any further decrease of the time scales $t_{1/2}$ and $t_{\lambda/2}$ suggests that the rate and anisotropy of crystallization in the outermost region are no longer sensitive to continued application of shear after some characteristic duration t_s*. Saturation of the kinetics and anisotropy of growth in the outermost region alone is not sufficient to explain the constancy of $t_{1/2}$ and $t_{\lambda/2}$; it would further require that the inner regions not produce substantial scattering on the same time scale (even a thickening of the region that contributes to scattering and birefringence would reduce $t_{1/2}$ and $t_{\lambda/2}$, which is not observed). One might speculate on the mechanism that could lead to such saturation behavior; perhaps there is some species that is consumed in producing the threadlike precursors which limits the extent of the flow-induced effect. Alternatively, the crystallites induced during flow might knit together, suppressing further deformation in a boundary layer near each wall, causing it to be insensitive to continued application of stress beyond that moment.

In contrast to the saturation behavior we observe in PP-300/6, Janeschitz-Kriegl and co-workers reported a power-law effect of t_s on crystallization time ($t_{\lambda/2} \sim t_s^{-2}$) throughout the range of conditions they imposed on an isotactic polypropylene of similar molecular weight and polydispersity (Daplen KS10, $M_n = 52\,000$ g/mol, $M_w = 330\,000$ g/mol).[23] There is evidence that such differences in behavior can result from subtle differences among similar materials. The Janeschitz-Kriegl group com-

pared two different Ziegler−Natta iPP samples, one with $M_n = 77\,000$ g/mol, $M_w = 235\,000$ g/mol, and $M_z = 545\,000$ g/mol and the other with $M_n = 47\,000$ g/mol, $M_w = 322\,000$ g/mol, and $M_z = 1\,360\,000$ g/mol.[24] The latter showed the $t_{\lambda/2} \sim t_s^{-2}$ scaling, while the former showed a weaker scaling ($t_{\lambda/2} \sim t_s^{-1}$ or even $t_{\lambda/2} \sim t_s^{0}$).[49] We do not believe the discrepancy between PP-300/6 and Daplen KS10 is due to the use of $t_{1/2}$ instead of using $t_{\lambda/2}$: in cases where both of these are observed, they follow the same trends as functions of t_s (Figure 5). We speculate that the difference between our observations ($t_{1/2}$ decreases initially with increasing t_s but saturates for $t_s > t_{crit}$) may be due to differences in the fraction and length of high molecular weight chains in the sample. It is possible that a molecular weight distribution with a stronger high molecular weight tail could delay the onset of saturation, if saturation is due to "consumption" of high molecular weight chains in the creation of oriented structures. This reiterates the importance of experiments with model systems to quantify the effect of the high molecular weight tail in the molecular weight distribution on shear-enhanced crystallization.

Implications Regarding Precursors to Oriented Crystallization. The development of an oriented skin in our ex situ morphological investigations correlates with the formation of oriented precursors during shear evident in the unusual upturn in the in situ birefringence signal upon flow start-up. Here we first discuss two models for flow-induced crystallization each of which captures the creation of oriented precursors during flow and their connection to subsequent development of oriented morphologies. We then contrast our findings to experimental observations of precursor structures that do not appear to play a role in our system.

The model of Doufas et al.[28] can capture a shear stress overshoot upon start-up of shear flow and the monotonic increase that follows. While the overshoot is a consequence of the nonlinear rheology of the amorphous melt, the subsequent upturn in shear stress results from the formation of crystallites. This parallels our observation of overshoot and subsequent upturn in the birefringence: the overshoot coming from the transient third normal stress difference and the upturn correlating with WAXD observations of oriented α-iPP crystallites.[44] However, the behavior in their model is crucially dependent on the choice of the empirical parameter that couples crystallization with amorphous orientation. A rational basis for an a priori choice of this parameter is currently lacking. Nevertheless, the strong nonlinear coupling in the model between crystallization kinetics and the orientation state of the crystallizing melt accords qualitatively with our observation that the emergence of precursors appears to be controlled by the time it takes for the melt to arrive at a given orientation state (Figure 9, as discussed below).

A physical (but phenomenological) picture for the generation of the precursors is suggested by the model proposed by Janeschitz-Kriegl to explain shear-enhanced crystallization. They postulate the formation of threadlike precursors during shear which grow from point nuclei with cylindrical symmetry, oriented in the flow direction. We believe that these threadlike precursors and the lamellae that grow out from them are manifested in the unusual rise in the birefringence and oriented WAXD patterns observed in our experiments in situ during shear for $\sigma_w > \sigma_{w,c}$ and $t_s > t_c(\sigma_w)$.

Amorphous precursors have been observed by McHugh and coworkers[50−52] during studies of seeded flow-induced crystallization of solutions of polyethylenes, isotactic polypropylenes, and polyethylene oxide. These liquidlike precursors form into oriented fibers for semicrystalline polymers. Since the precursors were also observed during flow of an atactic polystyrene system,[52] it was concluded that they originated from a liquid−liquid phase separation. We have examined the effect of extreme shearing conditions on an atactic polypropylene ($M_w = 217\,000$g/mol, PDI ≈ 2.3, conditions given in ref 53). No "shear-induced structure" was seen to form, suggesting that the birefringent feature we observe does not result from a liquid−liquid phase separation. Keller and co-workers[54] suggest that a coil−stretch transition (at stagnation points in an elongational field, or of polymer molecules adsorbed to the wall in a shear field) is necessary for creation of oriented crystalline structures. Such a transition would have a distinct signature characterized by a rise in the birefringence. Again, our experiments with the atactic sample show no evidence of a coil−stretch transition, which suggests that it is probably not necessary for the formation of an oriented skin layer. The "shear-induced structures" seen in our experiments most closely resemble the threadlike precursors proposed by Janeschitz-Kriegl.

Dynamics That Control the Formation of Oriented Structures. The effect of temperature on the development of the peculiar upturn in the birefringence during shear is quite surprising. With increasing temperature, the quiescent crystallization time increases strongly, due to the reduced subcooling. If the same physics played a significant role in determining the kinetics of formation of the highly oriented structures that form during flow, then they would form at later times with increasing temperature. Instead the opposite behavior is observed (Figure 9a): with increasing temperature, the upturn in the birefringence occurs at earlier times. This trend continues to hold even to temperatures above the melting point observed by hot stage microscopy! Interestingly, the temperature dependence is very close to that of the rheological time−temperature shift factor (solid curve, Figure 10). This strongly suggests that, while the "shear-induced structure" shows crystalline WAXD reflections,[44] its formation does not show the temperature dependence characteristic of a nucleated process. Rather, it appears to be strongly influenced by the dynamics of polymer chains in the melt. This temperature dependence is consistent with the rate-limiting step being the creation of a given orientational state of the melt. The stress level largely sets the magnitude of the anisotropy that will be reached; the time required to reach a given point in the transient orientation distribution after the flow start-up decreases with increasing temperature.

The fate of the oriented structures induced during shear is very sensitive to temperature in the vicinity of the observed melting point by DSC or hot stage microscopy. For temperatures of 160 °C or lower, the birefringence does not fully relax after cessation of flow and the birefringence that remains starts to grow as soon as relaxation is complete (Figure 11). At temperatures of 170 or 175 °C, the birefringence relaxes completely after cessation of flow. Experiments by McHugh and coworkers[32,48] on the crystallization of an HDPE droplet in planar extensional flow indicate that the development

of strong orientation in the system during flow relaxes after the cessation of flow for temperatures above the nominal melting point of the polymer (while for lower temperatures, this leads to the development of oriented crystallites). In addition, Sakellarides and McHugh[55] observed fibrillar crystals of HDPE at temperatures above the nominal melting point in the presence of localized, strong extensional gradients and found they were stable for a few minutes after cessation of flow and then melted gradually.

Synchrotron WAXD experiments performed at T_{cryst} around 140 to 150 °C,[44] prove that oriented crystallites produce the upturn in birefringence during flow at relatively large subcooling. The nature of the "shear-induced structure" at higher temperatures (e.g., $T = 170$ or 175 °C) is under investigation.

Implications of Shear-Induced Structures Formed above the Nominal Melting Point. A recent theory proposed by Janeschitz-Kriegl and co-workers[56,57] may provide insight into the "shear-induced structure" generated at high temperatures. They argue that the free energy penalty from classical nucleation theory associated with the formation of an interphase is a function of the size of nucleus, and goes to zero as the size decreases (leading to "athermal" nuclei). In the context of polymer crystallization, this surface free energy term physically represents the energy associated with fold surface at the amorphous−crystal interphase. On the basis of thermodynamic arguments, they estimate the upper bound for the formation of a stable athermal nucleus for iPP, $T_u \approx 170-180$ °C. Athermal nuclei formed below this temperature range are always stable, while they are metastable between T_u and the equilibrium melting temperature of the polymer. Our observations seem to accord well with this theory. The picture that emerges then is as follows: Upon shearing a polydisperse polymer melt below T_u, the high molecular weight chains in the melt are strongly distorted from their isotropic state. They can then form the "threadlike precursors" that grow off heterogeneities in the melt or the athermal nuclei. The fraction of high molecular weight chains might determine the concentration of the "threadlike precursors", which could account for the observed saturation behavior. At crystallization temperatures of 140 or 150 °C, crystalline structures might grow off the "threadlike precursors" in a very short time compared to the quiescent crystallization time ($>10^4$ s), giving rise to the observed crystalline diffraction spots that appear in a matter of a few seconds.[44] This explanation is also consistent with the temperature dependence of the time of formation of the "shear-induced structures". Further, it can be hypothesized that shearing the polymer melt increases T_u, and thus, at temperatures around to 170 °C, the athermal nuclei (and consequently the "shear-induced structures") may disappear upon cessation of shear.

The strong dependence of the "shear-induced structures" on rheological parameters suggests a direction for future studies to understand the molecular underpinnings of the "threadlike precursors" in the model of Janeschitz-Kriegl. Our results suggest that the "missing" time scale and the arbitrary critical shear strain rate in their model might be related to the rheological time scales of relaxation of the melt. Our data also suggest that the coupling parameters in the model of McHugh et al.[28] might depend on the chain length polydispersity of the system. Thus, further studies with binary blends of low polydispersity "long" and "short" chains might provide clues that could lead to a better understanding of the model parameters.

5. Conclusions

We have examined the shear-enhanced crystallization of a polydisperse isotactic polypropylene (PP-300/6). Shearing the polymer for a duration much shorter than the quiescent crystallization time at the crystallization temperature always led to significantly accelerated crystallization kinetics as compared to quiescent. However, when shearing above a critical stress was continued for a time greater than a critical duration, the acceleration of crystallization kinetics saturate and a transition to the formation of oriented structures occurs. An oriented, crystalline structure which we call the "shear-induced structure" is formed during shear when the wall shear stress is above some critical value and is applied for a critical shearing time. The formation of this "shear-induced structure" correlates with the subsequent formation of a skin-core semicrystalline morphology. The time at which the "shear-induced structure" appears decreases with temperature at fixed wall shear stress, governed by the rheology of the polymer melt and not by the subcooling.

Acknowledgment. We would like to acknowledge financial support from P&G, the Cargill-NIST ATP, NSF-DMR 9901403, and the Schlinger fund that made this project possible. One of the authors (K.G.) would like to acknowledge support from a Landau fellowship. We are very grateful to Dr. A. Prasad (Quantum Chemical) for providing us with the commercial grade polypropylene, PP8004MR ("PP-300/6"), for our experiments. We are grateful to Dr. R. L. Sammler (The Dow Chemical Co.) for providing us with the atactic polypropylene sample. We would also like to acknowledge help from Joanna Dodd for preliminary characterization of PP-300/6.

References and Notes

(1) Southern, J. H.; Porter, R. S. *J. Appl. Polym. Sci.* **1970**, *14*, 2305−2317.
(2) Odell, J. A.; Grubb, D. T.; Keller, A. *Polymer* **1978**, *19*, 617−626.
(3) Bashir, Z.; Odell, J. A.; Keller, A. *J. Mater. Sci.* **1984**, *19*, 3713−3725.
(4) Mencik, Z.; Fitchmun, D. R. *J. Polym. Sci. (Polym. Phys.)* **1973**, *11*, 973−989.
(5) Fitchmun, D. R.; Mencik, Z. *J. Polym. Sci. (Polym. Phys.)* **1973**, *11*, 951−971.
(6) Fujiyama, M.; Wakino, T.; Kawasaki, Y. *J. Appl. Polym. Sci.* **1988**, *35*, 29−49.
(7) Fujiyama, M.; Wakino, *T. J. Appl. Polym. Sci.* **1991**, *43*, 57−81.
(8) Isayev, A. I.; Chan, T. W.; Shimojo, K.; Gmerek, M. *J. Appl. Polym. Sci.* **1995**, *55*, 807−819.
(9) Lopez, L.; Cieslinski, R.; Putzig, C.; Wesson, R. *Polymer* **1995**, *36*, 2331−2341.
(10) Ulcer, Y.; Cakmak, M.; Miao, J.; Hsiung, C. *J. Appl. Polym. Sci.* **1996**, *60*, 669−691.
(11) Ulcer, Y.; Cakmak, M. *Polymer* **1997**, *38*, 2907−2923.
(12) Haas, T.; Maxwell, B. *Polym. Eng. Sci.* **1969**, *9*, 225−241.
(13) Kobayashi, K.; Nagasawa, T. *J. Macomol. Sci. (Phys.)* **1970**, *B4*, 331−345.
(14) Wereta, A., Jr.; Gogos, C. *Polym. Eng. Sci.* **1971**, *11*, 19−27.
(15) Lagasse, R.; Maxwell, B. *Polym. Eng. Sci.* **1976**, *16*, 189−199.
(16) Andersen, P.; Carr, S. *Polym. Eng. Sci.* **1976**, *16*, 217−221.
(17) Andersen, P.; Carr, S. *Polym. Eng. Sci.* **1978**, *18*, 215−221.
(18) Ulrich, R.; Price, F. *J. Appl. Polym. Sci.* **1976**, *20*, 1077−1093.
(19) Sherwood, C.; Price, F.; Stein, R. *J. Polym. Sci. (Polym. Symp.)* **1978**, *63*, 77−94.

(20) Wolkowicz, M. *J. Polym. Sci. (Polym. Symp.)* **1978**, *63*, 365−382.
(21) Tribout, C.; Monasse, B.; Haudin, J. *Colloid Polym. Sci.* **1996**, *274*, 197−208.
(22) Vleeshouwers, S.; Meijer, H. *Rheol. Acta* **1996**, *35*, 391−399.
(23) Liedauer, S.; Eder, G.; Janeschitz-Kriegl, H.; Jerschow, P.; Geymayer, W.; Ingolic, E. *Intern. Polym. Proc.* **1993**, *8*, 236−244.
(24) Jerschow, P.; Janeschitz-Kriegl, H. *Intern. Polym. Proc.* **1997**, *12*, 72−77.
(25) Ziabicki, A. *Colloid Polym. Sci.* **1974**, *252*, 207−221.
(26) Ziabicki, A. *Colloid Polym. Sci.* **1974**, *252*, 433−447.
(27) Bushman, A.; McHugh, A. *J. Polym. Sci. (Polym. Phys.)* **1996**, *34*, 2393−2407.
(28) Doufas, A. K.; Dairanieh, I. S.; McHugh, A. J. *J. Rheol.* **1999**, *43*, 85−109.
(29) Flory, P. J. *J. Chem. Phys.* **1947**, *15*, 397−408.
(30) Krigbaum, W.; Roe, R. *J. Polym. Sci. (A)* **1964**, *2*, 4391−4414.
(31) Mitchell, J. C.; Meier, D. J. *J. Polym. Sci. (A-2)* **1968**, *6*, 1689−1703.
(32) McHugh, A.; Guy, R.; Tree, D. *Colloid Polym. Sci.* **1993**, *271*, 629−645.
(33) Kumaraswamy, G.; Verma, R. K.; Kornfield, J. A. *Rev. Sci. Instr.* **1999**, *70*, 2097−2104.
(34) Shearing the polymer leads to a temperature increase due to viscous dissipation. However, the temperature increase is small since the shear rate is highest near the wall, which is maintained isothermal by the temperature control system and since the shear is imposed only for a brief duration. No variation in temperature during shear is recorded by a thermocouple positioned near the sample.
(35) The temperature chosen, 220 °C, was higher than the Hoffman−Weeks equilibrium melting temperature for PP-300/6, which was determined to be 190 °C. Holding at this temperature for 5 min was deemed to be adequate to erase melt memory effects since higher temperatures (up to 240 °C) or longer holding times did not have any measurable difference on the crystallization kinetics.
(36) The rise time is not limited by compression of the polymer in the reservoir, as determined by experiments with various ratios of reservoir-to-capillary volumes.[33] The time scale is not limited by the diffusion of momentum either: the time scale that governs the wall shear stress transient, τ_T, is on the order of w^2/ν, where w is the slit width and ν is the kinematic viscosity of the polymer melt, leading to $\tau_T \sim O(10^{-6}$ s) for the present experiments.
(37) Ma, Q.; Ishimaru, A.; Kuga, Y. *Radio Sci.* **1990**, *25*, 419−426.
(38) Nonlinear viscoelastic data obtained using a capillary rheometer indicate that PP-300/6 is shear thinning. Fitting this data to a power law model yields a value of about 0.38 for the power law exponent.
(39) Hot stage polarized light microscopy melting studies of quenched sections of PP-300/6 (T_{cryst} = 141 °C, σ_w = 0.06 MPa, t_{shear} = 12 s) show that the spherulitic core has a lower melting temperature than the oriented skin. This suggests that the core might have crystallized at a lower temperature than the skin.
(40) Janeschitz-Kriegl, H. *Polymer Melt Rheology and Flow Birefringence*; Springer-Verlag: New York, 1983.
(41) Larson, R. G. *Constitutive Equations for Polymer Melts and Solutions*; Butterworths: New York, 1988.
(42) Menezes, E.; Graessley, W. *J. Polym. Sci. (Polym. Phys.)* **1982**, *20*, 1817−1833.
(43) The trends showed by the birefringence on start up of flow (viz., initial overshoot followed by an upturn) might appear, at first glance, to be similar to those observed in shear stress by Wereta and Gogos[14] (Figure 6) or Andersen and Carr[17] (Figure 5). This is misleading. The steep increase in force and the subsequent decay between 10 and 20 s in Figure 6 of ref 14 is the viscoelastic response of the polymer melt to step strain. Neither the time scale nor the magnitude of the overshoot observed in the rheometer torque in Figure 5 of ref 17 change with the imposed strain rate, suggesting that the overshoot might be an artifact of the experimental setup (repositioning of the polymer, as suggested by the authors). In both these references, the increase in stress at later times results from an increase in modulus of the polymer due to crystallization with no evidence that these are oriented.
(44) Kumaraswamy, G.; Verma, R. K.; Wang, P.; Kornfield, J. A.; Yeh, F.; Hsiao, B. S. (in preparation) will present a complete analysis of our synchrotron SAXS and WAXD. The WAXD patterns obtained during shear at σ_w = 0.06 MPa and T_{cryst} = 141 °C for ∼6 s of shear are qualitatively similar to that in Figure 1a in the work of Andersen and Carr (Andersen, P. G. and Carr, S.H. *J. Mat. Sci.* **1975**, *10*, 870−886.) which was obtained from an iPP fiber with well-developed α-iPP crystal structure having strong uniaxial orientation of parent crystallites (*c* axis along the fiber), bearing the associated crosshatched "daughter" crystallites.
(45) Jones, A. T.; Aizlewood, J. M.; Beckett, D. R. *Makromol. Chem.* **1964**, *75*, 134−158.
(46) Ferry, J. D. *Viscoelastic Properties of Polymers*, John Wiley: New York, 3rd ed.; 1980.
(47) Eckstein, A.; Suhm, J.; Friedrich, C.; Maier, R.-D.; Sassmannshausen, J.; Bochmann, M.; Mulhaupt, R. *Macromolecules* **1998**, *31*, 1335−1340.
(48) Bushman, A. C.; McHugh, A. J. *J. Appl. Polym. Sci.* **1997**, *64*, 2165−2176.
(49) Figure 4 in ref 24.
(50) Rietveld, J.; McHugh, A. J. *J. Polym. Sci. (Polym. Lett.)* **1983**, *21*, 919−926.
(51) McHugh, A. J.; Blunk, R. H. *Macromolecules* **1986**, *19*, 1249−1255.
(52) McHugh, A.; Spevacek, J. *J. Polym. Sci. (Polym. Phys.)* **1991**, *29*, 969−979.
(53) Atactic polypropylene (M_r = 96 300 g/mol, M_w = 217 000 g/mol, M_z = 407 000 g/mol) was sheared at a temperature of 150 °C for shearing times of ∼20 s at wall shear stresses around 0.1 MPa. No upturn was seen in the birefringence observed during shear.
(54) Keller, A.; Kolnaar, H. W. H. Flow Induced Orientation and Structure Formation. In *Processing of Polymers*; Meijer, H. E. H., Ed.; VCH: NY, 1997; Vol. 18.
(55) Sakellarides, S. L.; McHugh, A. J. *Rheol. Acta* **1987**, *26*, 64−77.
(56) Janeschitz-Kriegl, H. *Colloid Polym. Sci.* **1997**, *275*, 1121−1135.
(57) Janeschitz-Kriegl, H.; Ratajski, E.; Wippel, H. *Colloid Polym. Sci.* **1999**, *277*, 217−226.

MA990772J